ACS APPLIED MATERIALS & INTERFACES

RESEARCH ARTICLE

www.acsami.org

High-Performance Triisopropylsilylethynyl Pentacene Transistors via Spin Coating with a Crystallization-Assisting Layer

Danbi Choi,[†,‡] Byungcheol Ahn,[†,§] Se Hyun Kim,[‡] Kipyo Hong,[‡] Moonhor Ree,[*,§] and Chan Eon Park[*,‡]

[‡]Polymer Research Institute, Department of Chemical Engineering, Pohang University of Science and Technology, Pohang, 790-784, Korea;

[§]Department of Chemistry, Division of Advanced Materials Science, Center for Electro-Photo Behaviors in Advanced Molecular Systems, Pohang Accelerator Laboratory, Polymer Research Institute, and BK School of Molecular Science, Pohang University of Science and Technology, Pohang, 790-794, Korea

ABSTRACT: The effects of spin speed and an amorphous fluoropolymer (CYTOP)-patterned substrate on the crystalline structures and device performance of triisopropylsilylethynyl pentacene (TIPS-PEN) organic field-effect transistors (OFETs) were investigated. The crystallinity of the TIPS-PEN film was enhanced by decreasing the spin speed, because slow evaporation of the solvent provided a sufficient time for the formation of thermodynamically stable crystalline structures. In addition, the adoption of a CYTOP-patterned substrate induced the three-dimensional (3D) growth of the TIPS-PEN crystals, because the patterned substrate confined the TIPS-PEN molecules and allowed sufficient time for the self-organization of TIPS-PEN. TIPS-PEN OFETs fabricated at a spin speed of 300 rpm with a CYTOP-patterned substrate showed a field-effect mobility of 0.131 $cm^2 V^{-1} s^{-1}$, which is a remarkable improvement over previous spin-coated TIPS-PEN OFETs.

KEYWORDS: triisopropylsilylethynyl pentacene (TIPS-PEN), crystallization-assisting layer, spin-coating, self-organization

INTRODUCTION

Organic field-effect transistors (OFETs), fabricated by solution-processing, have attracted significant attention because of their low operating temperatures, large areas, and ease of fabrication.[1−4] In particular, solution-processable triethylsilylethynyl anthradithiophene (TES-ADT) and poly(2,5-bis(3-alkylthiophen-2-yl)thieno-[3,2-b]thiophenes) (PBTTT) OFETs have been shown to exhibit high device performance comparable to that of OFET-containing, vacuum-deposited semiconducting films.[5−7]

To achieve high device-performance OFETs, it is essential to assemble a semiconductor layer with favorable molecular orientation and uniform morphology, both of which are decisive determinants of device- performance.[8,9] In recent solution-processed OFET developments, the formation of active layers via the selectively self-organized patterning technique has come into the spotlight.[10,11] This method allows semiconductor crystalline growth suitable for charge carrier transport in the patterned active regions by controlling of the solvent drying conditions and the surface wettability of the substrate. This technique results in high device performance and isolation between neighboring unit devices. Lee et al. reported the formation of a highly crystalline triisopropylsilylethynyl pentacene (TIPS-PEN) layer on a wettability-controlled substrate, resulting from control of the solvent evaporation rate.[11] In addition, an organic inverter with self-organized TIPS-PEN layers was recently demonstrated on a wettability-controlled substrate employing an amorphous fluoropolymer (CYTOP) polymer layer.[10] These studies have made a considerable contribution to the improvement of device performance via the drop-casting technique. However, they were limited in terms of the reproducibility of film formation.[12]

Spin-coating is a powerful film fabrication technique that can facilitate thin and uniform film formation.[13,14] In addition, it enables the evaporation of the solvent to be easily controlled by altering the spin speed during film formation,[15] which in turn affects the crystalline structure and the film morphology.[16] For example, a slow solvent evaporation rate gives sufficient time for TIPS-PEN molecules to be aligned with the ordered crystalline structure. However, spin-coated TIPS-PEN OFETs reported to date have shown low field-effect mobilities (μ, < 0.04 $cm^2 V^{-1} s^{-1}$), even with the use high boiling point solvents that led to slow evaporation rates.[9]

In this study, we investigate the self-organization behavior of TIPS-PEN molecules observed during spin-coating film formation, while varying the spin speed and patterning of the active layer. To demonstrate which film- fabrication factors induce molecular orientation and film morphology favorable to charge transport, optical microscopy (OM) and two-dimensional (2D) grazing incidence X-ray scattering (GIXS) were used. The findings confirmed that high performance TIPS-PEN OFETs can be obtained by optimizing the spin speed and by applying a selectively patterned substrate as a crystallization-assisting layer.

EXPERIMENTAL SECTION

For the fabrication of the OFETs, a heavily doped (100) Si wafer was used as the gate electrodes, and a thermally grown 300 nm thick layer of SiO_2 was used as the gate dielectric. To make a patterned layer in the desired substrate regions, we chose CYTOP as a patterning material (purchased from Asahi Glass and used without further purification).[17] The fabrication process for the patterning layer followed our previous work:[10] a 10 wt % CYTOP solution in its solvent (CT-solv. 180) was spin-coated on the SiO_2 gate dielectric (water contact angle, θ_{water}, of

Received: August 15, 2011
Accepted: September 30, 2011
Published: September 30, 2011

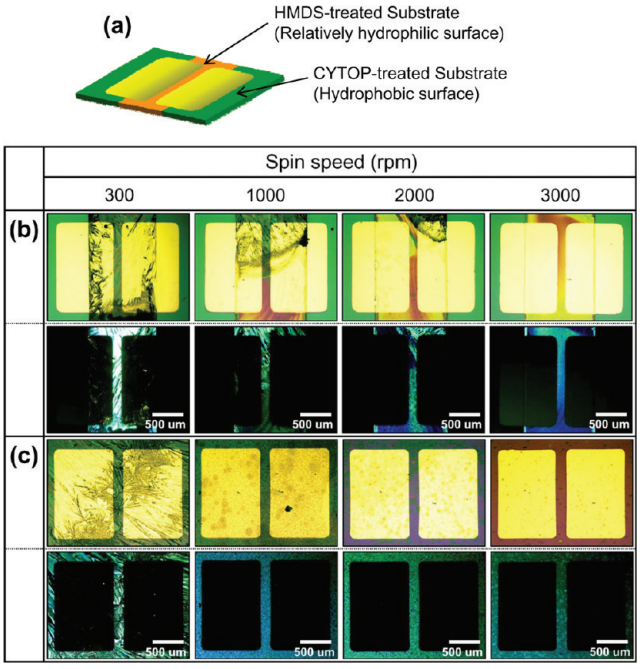

Figure 1. (a) Schematic illustration of selectively patterned substrate. Optical microscopy (OM) and polarized OM images of TIPS-PEN polycrystalline films made at various spin speeds on (b) patterned and (c) nonpatterned substrates.

ca. 108°) at 5000 rpm (rpm), followed by annealing for 20 min at 120 °C. The thickness of the CYTOP film, measured using an ellipsometer (J.A. Woollam. Co. Inc.), was ca. 20 nm. The patterned area was then easily obtained using oxygen plasma with a shadow mask, because the oxygen plasma cleared the C−F bonds in the CYTOP.[18] The CYTOP layer etched by the oxygen plasma (which were composed of SiO_2-) was completely removed[10] and the uncovered areas were treated with HMDS to change the hydrophilic SiO_2 surface to a hydrophobic surface (with θ_{water} of ca. 60°) that was less hydrophobic than the CYTOP areas (Figure 1a). The length (L) and width (W) of the patterned layer was 1000 and 2000 μm, respectively. Also nonpatterned substrates were equally treated with HMDS.

TIPS-PEN was used as an organic semiconductor.[19−23] TIPS-PEN was purchased from Polysis Co. A solution of TIPS-PEN (5 wt %) in toluene (boiling point (b.p.) = 110.6 °C) was spin-coated on the nonpatterned and patterned substrates at a various spin speeds of 300, 1000, 2000, and 3000 rpm. For the patterned substrates, TIPS-PEN molecules were only deposited onto the HMDS-treated areas, due to the dewetting properties of the CYTOP against common organic solvents. Gold source and drain electrodes (thickness 100 nm) were then defined on top of the semiconductor using a shadow mask. A channel L of 100 μm and a channel W of 1000 μm were obtained.

The electrical characteristics of the TIPS-PEN OFETs were determined using Keithley 2400 and 236 source/measure units under ambient conditions. Field-effect mobilities (μ) were extracted from plots of the square root of the drain-source current I_{DS} versus gate voltage (V_G) in the saturation regime ($V_{DS} = -40$ V), working from the equation $I_{DS} = (WC_i/2L)\mu(V_G - V_{th})^2$, where C_i is the capacitance per unit area of the gate dielectrics (10 nF/cm^2), and V_{th} is threshold voltage.

The TIPS-PEN film morphologies were characterized using polarized optical microscopy (POM) (Axioplan, Zeiss), and the microcrystalline structures of the TIPS-PEN thin films were investigated by 2D GIXS at the 4C2 beamline in the Pohang Accelerator Laboratory.[24−26] The

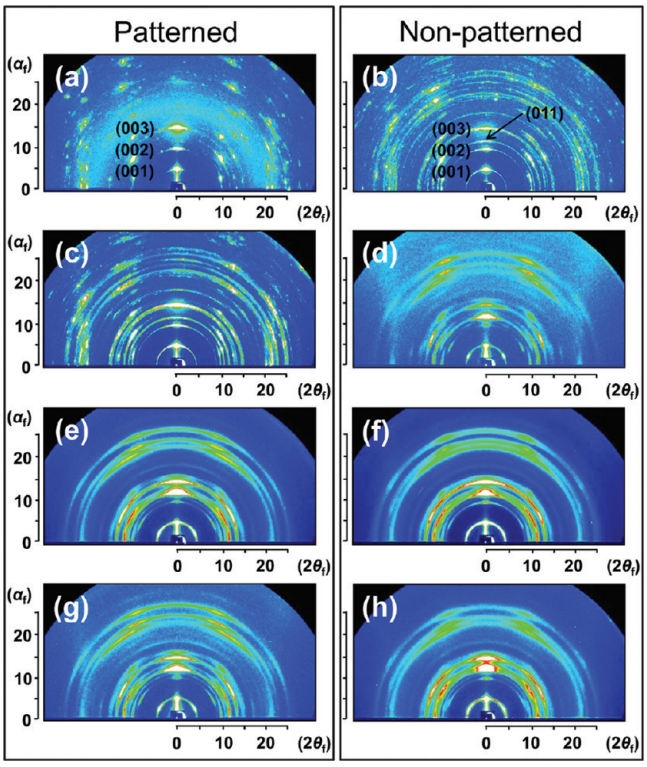

Figure 2. 2D GIXS patterns of TIPS-PEN thin films fabricated on nonpatterned and patterned substrates. The spin speeds were (a, b) 300, (c, d) 1000, (e, f) 2000, and (g, h) 3000 rpm.

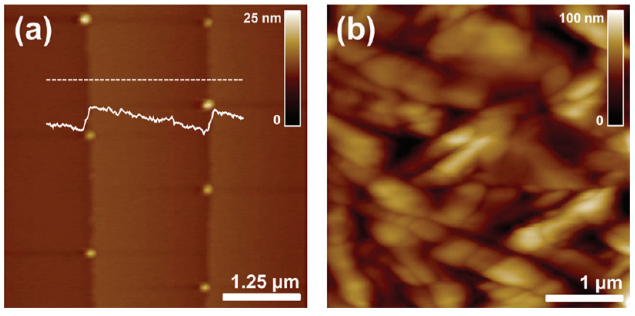

Figure 3. Height-mode AFM images of TIPS-PEN film on (a) 300 rpm, patterned, and (b) 300 rpm, nonpatterned substrate.

morphologies of the TIPS-PEN films were investigated using atomic force microscopy (AFM; Digital Instrument Multimode SPM) in tapping mode.

RESULTS AND DISCUSSION

Optical microscope (OM) and polarized OM images of the spin speed-dependent TIPS-PEN films grown on the CYTOP-patterned substrate are shown in Figure 1b. As the spin speed was increased from 300 to 3000 rpm, the TIPS-PEN film morphologies tended to change from an assembly of well-grown comb-shaped large crystals to featureless small crystals. Similarly, the crystal sizes increased with decreasing spin speed on the nonpatterned substrate (Figure 1c). However, unlike the well-ordered crystalline TIPS-PEN film on the patterned substrate generated at a spin speed of 300 rpm, the TIPS-PEN film on the

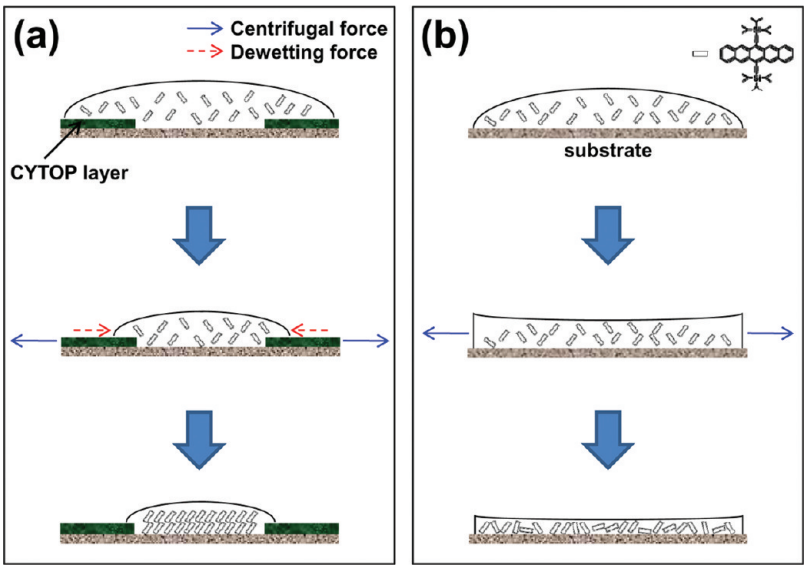

Figure 4. Schematic illustration of a possible mechanism for the formation of TIPS-PEN films on (a) nonpatterned and (b) patterned substrates.

Table 1. Average Values of Device Characteristics of TIPS-PEN OFETs on Nonpatterned and Patterned Substrates

rpm	substrate	μ (average) ($cm^2\ V^{-1}\ s^{-1}$)	I_{on}/I_{off}
300	nonpatterned	0.0111	1.21×10^5
	patterned	0.0725	1.88×10^5
1000	nonpatterned	0.0016	3.32×10^4
	patterned	0.0052	1.60×10^4
2000	nonpatterned	0.0015	3.36×10^3
	patterned	0.0021	2.72×10^3
3000	nonpatterned	0.0016	9.93×10^3
	patterned	0.0018	2.52×10^3

nonpatterned substrate clearly exhibited dendritic crystals, as well as a large number of boundaries between crystals that were randomly distributed throughout the substrate.

To provide further physical insight into the crystalline features and microstructural morphologies of the TIPS-PEN films developed with the each-patterned layer and various spin-speeds during film formation, we performed 2D GIXS (Figure 2) and AFM (Figure 3) analyses. The scattering pattern of the TIPS-PEN film fabricated at 300 rpm on the CYTOP-patterned substrate exhibited many scattering spots along the α_f, and the $2\theta_f$ directions, demonstrating well-ordered three-dimensional crystal in both lateral and vertical directions (Figure 2a).[27] AFM topography of TIPS-PEN film at 300 rpm also showed highly crystalline morphology with layer-by-layer structure, which verified the cross-sectional AFM profile in inset of Figure 3a. The *d*-spacing of layered crystals are approximately 16.8 Å, coinciding with the result of GIXS studies. On the other hand, scattering pattern of the TIPS-PEN film at 300 rpm on the nonpatterned substrate contained circular (001), (002), and (003) scattering patterns, which means that the crystals were randomly oriented on the substrate. Moreover, an intense (011) peak, corresponding to the pentacene ring of TIPS-PEN stacks in a direction perpendicular to the surface, was indicated, as shown in Figure 2b.[28] Similarly, large grains and randomly oriented crystalline morphology was observed on the nonpatterned substrate (Figure 3b). From these results, it was

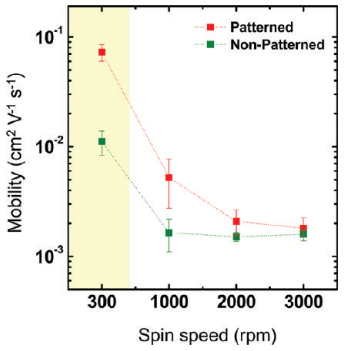

Figure 5. Variation of field-effect mobilities with respect to spin speeds on nonpatterned substrate and patterned substrate.

found that the CYTOP-patterned layer assisted the formation of well -ordered TIPS-PEN film structures during low spin speed coating. At high spin speeds (>1000 rpm), the intensity and positions of peaks appeared to be similar, regardless of the type of substrate (see Figure 2c–f). As the spin speed increased, remarkable and newly evolved multitudinous peaks such as (101) and (012) were increasingly observed in the circular scattering patterns (Figure 2g,h).[29] This indicated that the randomly oriented TIPS-PEN molecule structure content increased with increasing spin speed. It should be noted that structural defects such as crystal boundaries and misorientation are known to be charge traps that can induce current-resistance at the conducting channel.[30] In particular, it is very important to form a semiconductor assembly with optimal molecular orientation along the direction parallel to the charge-carrier path, as well as a packing structure that maximizes the degree of $\pi-\pi$ overlap, which is one of critical factors in determining the charge-carrier transport in π-conjugated organic semiconductors.[31] If a semiconductor film contains a non-negligible amount of film defects and crystals with molecular orientation unfavorable to the charge-carrier transport, the OFETs based on this semiconductor layer will yield decreased electrical performance compared with devices with well-ordered semiconductor structures.

dx.doi.org/10.1021/am201074n |*ACS Appl. Mater. Interfaces* 2012, 4, 117–122

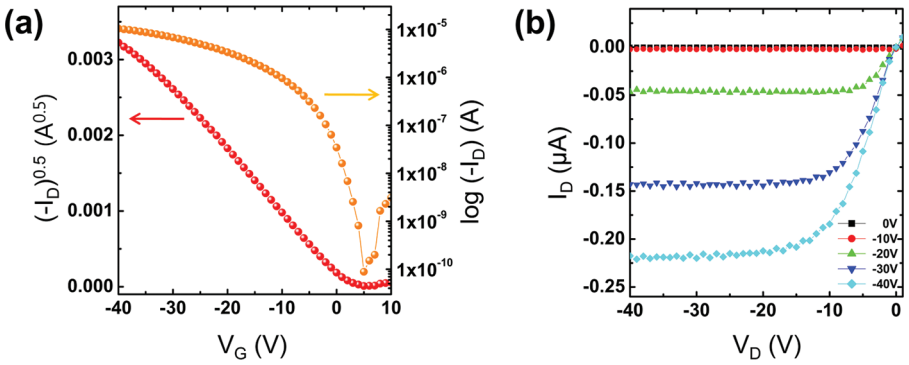

Figure 6. (a) I_D-V_G transfer characteristics and (b) I_D-V_D output characteristics (gate voltage, V_G = 0 to −40 V) for TIPS-PEN OFETs on patterned substrate.

The effects of spin speed and the CYTOP-patterned layer on the crystalline development of the TIPS-PEN were examined. We suggest that the behavior of these systems was determined by the evaporation rate of the solvent, because the semiconductor morphology is affected by the rate of solidification.[15] Previous works have shown that the molecular ordering of TIPS-PEN is determined to a large extent by the drying speed.[5,8,21,32] Slow solvent evaporation, produced by low spin speeds, enables the assembled TIPS-PEN molecules to approach their equilibrium state. As a result, thermodynamically preferred crystalline structures can be developed, which results in favorable molecular ordering and crystalline dimensions for high performance TIPS-PEN OFETs.[32] On the other hand, high spin speeds cause the fast solidification of the TIPS-PEN molecules, leading to film formation before the equilibrium state is reached. Hence, the TIPS-PEN film shows small crystals and unfavorable molecular orientation in reverse proportion to the spin speed, as described above.

Figure 4 shows that the CYTOP-patterned layer assisted the crystal formation of TIPS-PEN. On the CYTOP-patterned layer, the interface between the CYTOP layer and HMDS-treated area was able to act as an embankment to confine the TIPS-PEN solution, due to the difference in their wettabilities. During the low spin-speed coating (particularly at 300 rpm), the interfacial layer was able to prevent the spreading-out of the solution under the centrifugal force, thereby gaining time for the TIPS-PEN solution to self-organize. In addition, the TIPS-PEN crystals started to grow from the edge to the center in the patterned area, because the interface region functioned as a nucleation −site zone (Figure 4a).[33] Consequently, the resulting TIPS-PEN films showed large 3D comb-shaped crystals with molecular orientation favorable for charge transport. However, as the spin speed increased the centrifugal force was strong enough to overcome the embankment effect of the CYTOP-patterned layer. Without the patterned layer, a uniform TIPS-PEN film built up, but the crystal nuclei were randomly created over the whole substrate, showing limited self-organization of the TIPS-PEN film (Figure 4b).

To investigate the effects of the crystallization-assisting layer and the spin-speed on the charge transport of TIPS-PEN, we characterized the device performances from the top contact TIPS-PEN OFETs. The electrical parameters measured for the TIPS-PEN OFETs (such as μ, and on/off ratio (I_{on}/I_{off})) are summarized in Table 1. The TIPS-PEN OFETs made at high spin speed showed low μ values on both substrates; the values of μ were almost identical, and of the order of 10^{-3} cm^2 V^{-1} s^{-1}

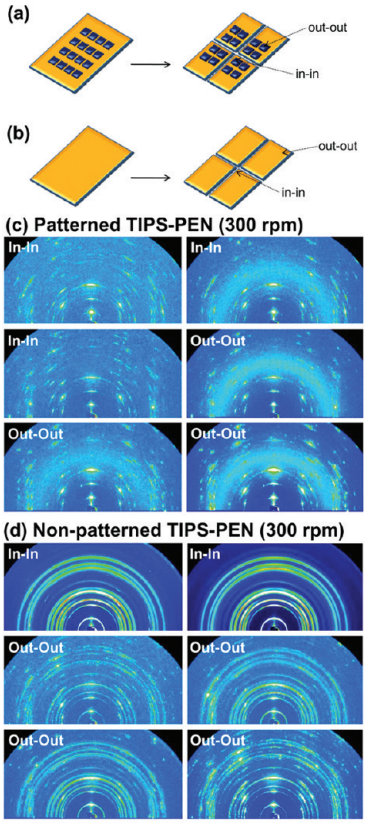

Figure 7. Schematic representation of partially divided samples with respect to the positions on (a) patterned and (b) nonpatterned substrates. 2D GISX patterns of TIPS-PEN films on (c) patterned substrate and (d) nonpatterned substrate made at a spin speed of 300 rpm.

(Figure 5). The μ and I_{on}/I_{off} values increased with decreasing spin speed. In particular, patterned TIPS-PEN OFETs made at 300 rpm showed high μ values, as expected from the 2D GIXS results. From the transfer curve of the device in Figure 5a, the average μ value was 0.0725 cm^2 V^{-1} s^{-1}, with a maximum of 0.131 cm^2 V^{-1} s^{-1} and an I_{on}/I_{off} yield above 1×10^5. The output curve showed a clear transition from linear to saturation behavior (Figure 6b). These device performance characteristics were comparable to those of amorphous silicon transistors and better than those of TIPS-PEN OFETs fabricated by spin-coating processes,

even in the higher b.p. solvent chlorobenzene, (b.p. of 131.7 °C, μ of 0.04 $cm^2 V^{-1} s^{-1}$.[9] In general, slower solvent evaporation generates more structural rearrangement prior to film solidification, because of sufficient available time for self-organization among the molecules. Interestingly, faster-evaporating toluene yielded superior device performance compared to OFETs made using slower-evaporating chlorobenzene, supporting the usefulness of CYTOP-patterned layer. Moreover, the difference in μ between patterned and nonpatterned devices (made at the same spin speed) gradually increased as the spin speed decreased, showing that the patterned device performed more effectively when manufactured at low spin speeds.

Further study is needed to evaluate the suitability of the patterning layer as a crystallization-assisting layer, especially with regard to reproducibility for film formation. Two TIPS-PEN films formed at 300 rpm on patterned and nonpatterned substrates were split into small pieces: the outermost and the innermost pieces are named out-out and in-in, respectively (see Figure 7a,b). The microstructural crystallinity and orientation of the films were investigated with 2D GIXS. As a result, identical scattering patterns for both the crystallinity and the orientation were observed on the patterned substrate (Figure 7c). However, rather different scattering patterns in the intensity and positions of peaks were verified on the nonpatterned substrate (Figure 7d).

CONCLUSION

In conclusion, we have demonstrated that a selectively patterned CYTOP layer assists the crystallization of TIPS-PEN in forming well-ordered crystalline structures during spin coating. OM and POM images showed that the crystallization of TIPS-PEN was enhanced by decreasing the spin speed. Based on the GIXS result, we verified that well-stacked 3D crystals were formed on the patterned substrate, while various-sized anisotropic crystalline structures evolved on the nonpatterned substrate. High-performance TIPS-PEN OFETs could be obtained by applying a low spin speed and the crystallization-assisting layer simultaneously. The optimized device showed a μ value as high as 0.131 $cm^2 V^{-1} s^{-1}$ and an on/off current ratio of 1×10^5. We believe that the use of a crystallization-assisting layer is a practical way to facilitate the commercial availability of solution-processed OFETs, and to ensure the reproducibility of the crystallinity and the orientation.

AUTHOR INFORMATION

Corresponding Author

*Tel: +82-54-279-2269 (C.E.P.); +82-54-279-2120 (M.R.). Fax: +82-54-279-8298 (C.E.P.); +82-54-279-3399 (M.R.). E-mail: cep@postech.edu (C.E.P.); ree@postech.edu (M.R.).

Author Contributions

†Danbi Choi and Byungcheol Ahn contributed equally to this work.

ACKNOWLEDGMENT

This study was supported by the National Research Foundation of Korea (Grant 20110000330 and Center for Electro-Photo Behaviors in Advanced Molecular Systems (2010-0001784)) and of the Ministry of Education, Science & Technology (MEST) (BK21 Program and World Class University Program (R31-2008-000-10059-0)). The synchrotron X-ray scattering measurements at Pohang Accelerator Laboratory were supported by MEST, POSCO, and POSTECH Foundation.

REFERENCES

(1) Halik, M.; Klauk, H.; Zschieschang, U.; Schmid, G.; Dehm, C.; Schutz, M.; Maisch, S.; Effenberger, F.; Brunnbauer, M.; Stellacci, F. *Nature* **2004**, *431*, 963.

(2) Sekitani, T.; Takamiya, M.; Noguchi, Y.; Nakano, S.; Kato, Y.; Sakurai, T.; Someya, T. *Nat. Mater.* **2007**, *6*, 413.

(3) Newman, C. R.; Frisbie, C. D.; da Silva, D. A.; Bredas, J. L.; Ewbank, C. P.; Mann, K. R. *Chem. Mater.* **2004**, *16*, 4436.

(4) Liu, S.; Briseno, A. L.; Mannsfeld, S. C. B.; You, W.; Locklin, J.; Lee, H. W.; Xia, Y.; Bao., Z. *Adv. Funct. Mater.* **2007**, *17*, 2891.

(5) Payne, M. M.; Parkin, S. R.; Anthony, J. E.; Kuo, C.; Jackson, T. N. *J. Am. Chem. Soc.* **2005**, *127*, 4986.

(6) Dickey, K. C.; Anthony, J. E.; Loo, Y.-L. *Adv. Mater.* **2006**, *18*, 1721.

(7) McCulloch, I.; Heeney, M.; Bailey, C.; Genevicius, K.; Macdonald, I.; Shkunov, M.; Sparrowe, D.; Tierney, S.; Wagner, R.; Zhang, W.; Chabinyc, M. L.; Kline, R. J.; McGehee, M. D.; Toney, M. F. *Nat. Mater.* **2006**, *5*, 328.

(8) Park, S. K.; Jackson, T. N.; Anthony, J. E.; Mourey, D. A. *Appl. Phys. Lett.* **2007**, *91*, 063514.

(9) Kim, Y.-H.; Lee, Y. U.; Han, J.-I.; Han, S.-M.; Han, M.-K. *J. Electrochem. Soc.* **2007**, *154*, H995.

(10) Kim, S. H.; Choi, D.; Chung, D. S.; Yang, C.; Jang, J.; Park, C. E.; Park, S.-H. K. *Appl. Phys. Lett.* **2008**, *93*, 113306.

(11) Lee., H. S.; Kwak, D.; Lee, W. H.; Cho, J. H.; Cho, K. *J. Phys. Chem. C.* **2010**, *114*, 2329.

(12) Mang, M.; Bao, Z. *Chem. Mater.* **2004**, *16*, 4824.

(13) Wu, P.-Y.; Chou, F.-C. *J. Electrochem. Soc.* **1999**, *146*, 3826.

(14) Schwartz., L. W.; Roy, R. V. *Phys. Fluids.* **2004**, *16*, 569.

(15) Meyerhofer, D. *J. Appl. Phys.* **1978**, 3993.

(16) Delongchamp, D. M.; Vogel, B. M.; Jung, Y.; Gurau, M. C.; Richter, C. A.; Kirillov, O. A.; Obrzut, J.; Fischer, D. A.; Sambasivan, S.; Richter, J.; Lin, E. K. *Chem. Mater.* **2005**, *17*, 5610.

(17) Kim, S.-J.; Ahn, T.; Suh, M. C.; Yu, C.-J.; Kim, D. W.; Lee, S.-D. *Jpn. J. Appl. Phys. Part 2.* **2005**, *44*, L1109.

(18) Griscom, L.; Degenaar, P.; LePioufle, B.; Tamiya, E.; Fujita, H. *Sens. Actuators, B* **2002**, *83*, 15.

(19) Park, S. K.; Anthony, J. E.; Jackson *IEEE Electron. Device Lett.* **2007**, *28*, 877.

(20) Nam, S.; Chung, D. S.; Jang, J.; Kim, S. H.; Yang, C.; Kwon, S.-K.; Park, C. E. *J. Electrochem. Soc.* **2010**, *125*, H90.

(21) Lim, J. A.; Lee, W. H.; Lee, H. S.; Lee, J. H.; Park, Y. D.; Cho, K. *Adv. Funct. Mater.* **2008**, *18*, 229.

(22) Anthony, J. E.; Brooks, J. S.; Eaton, D. L.; Parkin, S. R. *J. Am. Chem. Soc.* **2001**, *123*, 9482.

(23) Minari, T.; Kano, M.; Miyadera, T.; Wang, S.-D.; Aoyagi, Y.; Seto, M.; Nemoto, T.; Isoda, S.; Tsukagoshi, T. *Appl. Phys. Lett.* **2008**, *92*, 173301.

(24) Lee, B.; Park, Y.-H.; Hwang, Y.; Oh, W.; Yoon, J.; Ree, M. *Nat. Mater.* **2005**, *4*, 147.

(25) Lee, B.; Oh, W.; Hwang, Y.; Park, Y.-H.; Yoon, J.; Jin, K. S.; Heo, K.; Kim, J.; Kim, K.-W.; Ree, M. *Adv. Mater.* **2005**, *17*, 696.

(26) Yoon, J.; Kim, K.-W.; Kim, J.; Heo, K.; Jin, K. S.; Jin., S.; Shin, T. J.; Lee, B.; Rho, Y.; Ahn, B.; Ree, M. *Macromol. Res.* **2008**, *16*, 575.

(27) Yoon, D. K.; Yoon, J.; Kim, Y. H.; Choi, M. C.; Kim, J.; Sakata, O.; Kimura, S.; Kim, M. W.; Smalyukh, I. I.; Clark, N. A.; Ree, M.; Jung, H.-T. *Phys. Rev. E* **2010**, *82*, 041705.

(28) Kim, D. H.; Lee, D. Y.; Lee, H. S.; Lee, W. H.; Kim, Y. H.; Han, J. I.; Cho, K. *Adv. Mater.* **2007**, *19*, 678.

(29) Chen, J.; Anthony, J.; Martin, D. C. *J. Phys. Chem. B.* **2006**, *110*, 16397.

(30) Choi, D.; Jin, S.; Lee, Y.; Kim, S. H.; Chung, D. S.; Hong, K.; Yang, C.; Jung, J.; Kim, J. K.; Ree, M.; Park, C. E. *ACS Appl. Mater. Interfaces* **2010**, *2*, 48.

(31) Sirringhaus, H.; Brown, P. J.; Friend, R. H.; Nielsen, M. M.; Bechgaard, K.; Langeveld-Voss, B. M. W.; Spiering, A. J. H.; Janssen, R. A. J.; Meijer, E. W.; Herwig, P.; de Leeuw, D. M. *Nature* **1999**, *401*, 685.
(32) Kim, C. S.; Lee, S.; Gomez, E. D.; Anthony, J. E.; Loo, Y.-L. *Appl. Phys. Lett.* **2008**, *93*, 103302.
(33) Park, J. H.; Lee, K. H.; Mun, S.-J.; Ko, G.; Heo, S. J.; Kim, J. H.; Kim, E.; Im, S. *Org. Electron.* **2010**, *11*, 1688.